Research Square

Preprints are preliminary reports that have not undergone peer review.
They should not be considered conclusive, used to inform clinical practice,
or referenced by the media as validated information.

Annual maximum daily precipitation in the Central Chernozem Region of European Russia, 1936–2025: weak trends and their implications for regional design rainfall

Anna Naumova

koshevaya81@mail.ru

Russian State Agrarian University – Moscow Timiryazev Agricultural Academy

Research Article

Keywords: Precipitation extremes, Rx1day, Field significance, Regional frequency analysis, L-moments, European Russia

Posted Date: October 26th, 2026

DOI: https://doi.org/10.21203/rs.3.rs-11253647/v1

License: This work is licensed under a Creative Commons Attribution 4.0 International License. Read Full License

Additional Declarations: No competing interests reported.

Abstract

Annual maximum daily precipitation (Rx1day) controls soil erosion on the loess uplands of the Central Chernozem Region of European Russia and the design of drainage structures, yet regional evidence on its long-term behaviour is limited. We analysed Rx1day at 25 stations for 1960–2025 and at 12 stations back to 1936, using the Mann–Kendall test corrected for serial correlation, a permutation test of field significance, and L-moment frequency analysis with the generalised extreme value and Pearson type III distributions at individual sites and with the Hosking–Wallis regional index procedure. Theil–Sen slopes for 1960–2025 are positive at 14 stations, zero at six and negative at five; the regional median is + 0.2 mm per decade (0.6% of the mean), no station is significant at the 5% level, and the ensemble is not field-significant. A weak but more coherent increase appears in the cold season. The 1936–2025 series fluctuate by about ± 6% between decades around a nearly constant level. At-site 100-year estimates range from 60 to 123 mm, with 90% bootstrap intervals of about ± 19%; regional estimation narrows the range to 75–99 mm and the intervals to about ± 8%. Changes in the 100-year quantile implied by the observed trends (median below 1 mm) are an order of magnitude smaller than this uncertainty. Stationary regional estimates with explicit uncertainty bounds therefore appear adequate for design; the absence of a detectable trend reflects the limited power of 60-year records rather than evidence that extremes are not changing.

1 Introduction

The largest daily precipitation total of the year (Rx1day; Zhang et al. 2011) is a compact descriptor of the rainfall events that matter most for land and water management. In the Central Chernozem Region (CCR) of European Russia – a forest-steppe belt of deeply dissected loess uplands with some of the most fertile and intensively cultivated soils in Eurasia – a single heavy downpour on bare or freshly sown slopes can remove more topsoil than a season of moderate rain, feed the dense gully network and overload culverts, storm drains and small retention structures designed for historical conditions (Nearing et al. 2004; Litvin et al. 2017; Mal'tsev and Yermolaev 2020). In the small catchments of the region the maximum discharge responds to changes in storm rainfall and in land use together, and separating the two influences requires reliable statistics of the rainfall input itself (Ilinich et al. 2020, 2023). Design rainfall depths of a given return period are therefore a routine input in engineering practice, where they are usually derived from annual maximum series under the assumption of stationarity (SP 33-101-2003).

Globally, annual maximum daily precipitation has increased at a majority of stations with long records, broadly in line with the growth of atmospheric moisture content under warming (Westra et al. 2013; Donat et al. 2016; Papalexiou and Montanari 2019; Sun et al. 2021; Fowler et al. 2021). For Russia, national assessments report a rising contribution of heavy and convective precipitation to seasonal totals (Groisman et al. 2005; Zolina et al. 2010; Chernokulsky et al. 2019; Roshydromet 2022), and a positive dependence of extreme precipitation on temperature has been documented from station and reanalysis data (Aleshina et al. 2021). It would be natural to expect the same tendency in the CCR. However, the region lies in a transition zone between the humid centre of the East European Plain and the semi-arid south, where summer precipitation has shown little change or a decrease in recent decades and where warm-season extremes are produced by a small number of convective events with strong local variability. Conclusions drawn from

national or continental analyses, which rely on coarse station selections or gridded products, cannot be transferred to such a region without verification against complete local records.

Two methodological points make regional verification delicate. First, annual maxima are noisy: physically plausible trends of a few per cent per decade may remain undetectable at individual stations over six or even nine decades, and the question of whether an ensemble of weak, same-signed station trends constitutes a regional signal requires a formal test of field significance that accounts for the spatial dependence between stations (Livezey and Chen 1983; Wilks 2006, 2016). Second, design values for return periods of 50–100 years estimated from single-station records of about 60 years carry a large sampling uncertainty that is rarely reported, and their sensitivity to the choice of distribution and to possible non-stationarity is seldom compared with that uncertainty (Katz et al. 2002; Serinaldi and Kilsby 2015). Regional frequency analysis based on L-moments (Hosking and Wallis 1997) offers a way to reduce the sampling component, but it has rarely been applied to precipitation extremes in European Russia, where the Pearson type III distribution fitted by conventional moments remains the standard (SP 33-101-2003).

This study examines annual maximum daily precipitation at 25 stations of the CCR for 1960–2025 and at 12 stations for 1936–2025. Its objectives are (i) to quantify long-term changes in Rx1day for the whole year and separately for the warm and cold seasons, and to test whether these changes are field-significant at the regional scale; (ii) to estimate design daily precipitation for return periods of 10–100 years at individual sites and by the regional index procedure, with an explicit assessment of sampling and distributional uncertainty; and (iii) to compare the changes in design values implied by the observed trends with the uncertainty of the estimates themselves. The analysis is deliberately kept close to the data and to methods that are standard in climatology and hydrology, so that the results can be reproduced and updated as the records lengthen.

2 Study area and data

2.1 Study area

The CCR occupies the central part of the East European Plain between about 50° and 53.5° N and 34.5° and 43° E and comprises the Belgorod, Voronezh, Kursk, Lipetsk and Tambov administrative regions (about 168 000 km²; Fig. 1). The western and central parts lie on the Central Russian Upland (station elevations up to 274 m a.s.l.), the eastern part on the Oka–Don Lowland (86–150 m). The surface is formed by loess and loess-like loams on which chernozems and grey forest soils have developed; the uplands are dissected by a dense network of ravines and gullies. The climate is temperate continental, with a mean annual air temperature of about 6–8°C and annual precipitation decreasing from about 600 mm in the north-west to about 450 mm in the south-east, with a summer maximum. Heavy daily rainfall is almost entirely a warm-season phenomenon associated with convective systems, often embedded in frontal zones. Arable land occupies more than 60% of the territory and forest less than 10%, so that most slopes are exposed to rainfall during the convective season.

2.2 Data

Monthly maxima of daily precipitation totals at stations of the Russian Hydrometeorological Service (Roshydromet) were compiled from the archive of the All-Russian Research Institute of Hydrometeorological

Information – World Data Centre (RIHMI-WDC; Bulygina et al. 2014), accessed through its open data service, and the largest values were cross-checked against the primary archive. Daily totals at Russian stations are measured with the Tretyakov gauge, and the archived values include the standard wetting correction (Groisman et al. 1991). Values are reported to the nearest millimetre.

Of 31 stations with monthly maxima available for the region, 25 have records beginning in 1960 or earlier (Liski from 1966) and were retained; six stations whose observations begin between 2000 and 2011 were excluded. Twelve of the 25 stations have records from 1936 or earlier and were used for a longer analysis (Table 1). The annual maximum (Rx1day) of a calendar year was taken as the largest of the twelve monthly maxima; a year was accepted only when all months from April to October were present, because almost all annual maxima fall in this interval. Isolated zero values in the year 2000, which evidently represent missing data rather than observations, were removed. The resulting dataset for 1960–2025 contains 1557 station-years, with 53–66 accepted years per station (80–100% of the period). Seasonal maxima were formed in the same way for the warm (April–October) and cold (November–March) seasons. The year 2026 was incomplete at the time of analysis and was not used.

Table 1

Meteorological stations of the Central Chernozem Region used in the study and characteristics of annual maximum daily precipitation (Rx1day), 1960–2025. n – number of accepted years; CV – coefficient of variation; Max – largest recorded daily total (year). Stations with records from 1936 or earlier (used in Section 4.5) are marked with an asterisk

No.	Station	Region	Lat, °N	Lon, °E	Alt, m	Record from	n	Mean, mm	CV	Max, mm (year)
1	Anna*	Voronezh	51.50	40.41	152	1936	59	35.9	0.38	89 (1967)
2	Belgorod*	Belgorod	50.65	36.58	223	1936	57	37.3	0.28	65 (1979)
3	Bogoroditskoye*	Belgorod	51.16	37.35	223	1890	66	35.4	0.27	65 (2011)
4	Boguchar*	Voronezh	49.94	40.55	86	1936	64	34.8	0.41	83 (1963)
5	Borisoglebsk	Voronezh	51.36	42.11	104	1959	58	37.2	0.34	81 (1980)
6	Valuyki*	Belgorod	50.21	38.09	111	1936	66	39.0	0.37	87 (1989)
7	Voronezh*	Voronezh	51.72	39.22	147	1918	66	35.3	0.35	95 (1988)
8	Gotnya*	Belgorod	50.80	35.76	225	1936	66	36.2	0.39	82 (1973)
9	Yelets	Lipetsk	52.60	38.56	167	1959	64	37.1	0.41	89 (2025)
10	Zherdevka	Tambov	51.83	41.45	145	1955	64	34.5	0.39	78 (1976)
11	Kalach	Voronezh	50.41	41.05	90	1959	66	34.0	0.53	117 (2021)
12	Kamennaya Step*	Voronezh	51.05	40.72	193	1893	66	32.8	0.29	57 (1981)
13	Kirsanov	Tambov	52.66	42.71	169	1959	59	35.3	0.38	71 (1961)
14	Kon-Kolodez*	Lipetsk	52.15	39.16	138	1893	66	34.4	0.32	72 (1999)
15	Kursk*	Kursk	51.77	36.17	246	1891	66	38.3	0.37	88 (2000)
16	Lipetsk	Lipetsk	52.70	39.53	176	1939	59	33.7	0.35	77 (1982)
17	Liski	Voronezh	50.99	39.51	114	1966	53	32.5	0.36	74 (1989)

No.	Station	Region	Lat, °N	Lon, °E	Alt, m	Record from	n	Mean, mm	CV	Max, mm (year)
18	Michurinsk*	Tambov	52.88	40.48	148	1882	59	36.9	0.43	80 (1984)
19	Morshansk	Tambov	53.44	41.78	143	1959	59	33.2	0.37	71 (2023)
20	Novy Oskol	Belgorod	50.74	37.89	139	1959	60	37.5	0.38	86 (2013)
21	Oboyan	Kursk	51.20	36.32	190	1959	59	37.2	0.38	71 (2013)
22	Ponyri	Kursk	52.32	36.31	274	1959	66	42.8	0.42	83 (1969)
23	Rylsk	Kursk	51.55	34.69	205	1959	66	40.7	0.35	84 (1989)
24	Stary Oskol	Belgorod	51.32	37.77	216	1951	57	39.4	0.49	108 (1996)
25	Tambov*	Tambov	52.80	41.49	127	1936	66	33.7	0.33	72 (1998)

Because the data are integer millimetres, ties are frequent. This affects rank-based statistics only marginally, but it means that the Theil–Sen slope can be exactly zero where the signal is weak; we note this where relevant.

3 Methods

3.1 Homogeneity

Each annual series was tested for a single change-point in the mean with the Pettitt (1979) test, the standard normal homogeneity test (Alexandersson 1986) and the Buishand (1982) range test at the 5% level. Series flagged by all three tests were retained but are interpreted with caution; no adjustment was applied, because the available metadata do not identify the cause of the shift.

3.2 Trend analysis

Monotonic trends were tested with the non-parametric Mann–Kendall test (Mann 1945; Kendall 1975) using the variance correction of Hamed and Rao (1998) for serial correlation (Yue et al. 2002b). Trend magnitude was estimated by the Theil–Sen slope (Theil 1950; Sen 1968) and expressed in mm per decade and as a percentage of the 1960–2025 station mean. Two-sided tests at the 5% and 10% levels were used, and p-values are reported in full rather than as binary outcomes. The same procedure was applied to the annual, warm-season and cold-season series for 1960–2025 and to the annual series for 1936–2025 at the 12 long-record stations.

3.3 Field significance and regional series

The chance of finding a given number of positive or locally significant trends among 25 stations depends on how strongly the stations are correlated. Field significance was therefore assessed with a permutation test in which calendar years were shuffled as whole cross-sections, so that all stations receive the same permuted order of years; this preserves the spatial dependence of the data while removing any temporal trend (Livezey and Chen 1983). For each of 1000 permutations four statistics were recomputed: the number of positive Theil–Sen slopes, the difference between the numbers of positive and negative slopes, the number of stations significant at the 10% level, and the slope of a regional series. The field p-value is the fraction of permutations with a statistic at least as extreme as the observed one. The regional series is the mean over stations of annual Rx1day divided by the station mean for 1960–2025; this normalisation gives each station equal weight and limits the influence of varying station availability.

3.4 Detection power

To place the station tests in context, the probability of detecting a linear trend with the Mann–Kendall test was estimated for series of 64 years generated from the regional distribution of Rx1day (Section 3.6) with imposed slopes of 0.5, 1, 2 and 3 mm per decade (1000 realisations per slope; cf. Yue et al. 2002a).

3.5 At-site frequency analysis

Design daily precipitation for return periods T = 10, 50 and 100 years was estimated at each station from the annual series with the generalised extreme value (GEV) distribution, which is the asymptotic form for block maxima (Coles 2001), and with the Pearson type III (PE3) distribution, which is standard in Russian practice (SP 33-101-2003). Parameters of both were estimated by L-moments (Hosking 1990), which are considerably less sensitive to the sampling variability of skewness than conventional moments for series of this length; PE3 was also fitted by the method of moments for comparison with national practice. Goodness of fit was checked with the Kolmogorov–Smirnov test and with the position of the sample L-skewness and L-kurtosis relative to the theoretical curves on the L-moment ratio diagram. Sampling uncertainty of the quantiles was quantified as the 5–95% range of 1000 non-parametric bootstrap replicates of each series.

3.6 Regional frequency analysis

The index procedure of Hosking and Wallis (1997) was applied with the station mean as the index variable. The discordancy measure Di was computed for each site (critical value 3.0 for 25 sites); the heterogeneity measures H1 (based on the dispersion of L-CV), H2 (L-CV and L-skewness) and H3 (L-skewness and L-kurtosis) were obtained from 1000 simulations of a four-parameter kappa distribution fitted to the regional average L-moment ratios; and the goodness-of-fit measure ZDIST was evaluated for the generalised logistic, GEV, generalised normal and PE3 distributions, with $|Z| \le 1.64$ taken as acceptable. The regional growth curve was then derived from the regional L-moments, and site quantiles were obtained as the product of the growth factor and the station mean. The procedure was repeated for the 24 sites remaining after removal of the most discordant station and for the subset of 22 sites obtained by removing the three most discordant stations. The uncertainty of the growth factors and of the site quantiles was quantified with 1000 bootstrap replicates of the pooled data, repeating the full procedure in each replicate. The heterogeneity measure assumes independent sites; cross-correlation inflates it only moderately (Castellarin et al. 2008), and the weak dependence among the stations (Section 4.1) is unlikely to affect its interpretation.

3.7 Sensitivity of design values to the observed changes

Two simple experiments were used to express the observed trends in terms of design values. First, GEV quantiles were re-estimated separately from the first (1960–1992) and second (1993–2025) halves of each record. Second, a GEV with a location parameter varying linearly in time was fitted by maximum likelihood, the improvement over the stationary model was judged by a likelihood-ratio test, and the effective 100-year value was evaluated for 1960 and 2025. These experiments are diagnostic; no extrapolation beyond the observation period was attempted.

4 Results

4.1 Climatology of annual maximum daily precipitation

The long-term mean Rx1day for 1960–2025 ranges from 32.5 mm (Liski) to 42.8 mm (Ponyri), with a regional average of 36.2 mm (Table 1); no clear spatial gradient is apparent, and the differences between neighbouring stations are of the same size as those across the region. The series are strongly right-skewed (sample skewness 0.5–2.5) with coefficients of variation of 0.27–0.53. The largest recorded daily totals – 117 mm at Kalach (2021), 108 mm at Stary Oskol (1996) and 100 mm at Kalach (1974) – exceed the station means roughly threefold; only 23 of 1557 station-years (1.5%) reached 80 mm. About 61% of the annual maxima occurred in June–August, with a peak in July (24%); 93% occurred between April and October, and the cold season contributes 7%. Cold-season maxima average 15–21 mm, roughly half the warm-season values.

The correlation between annual maxima at different stations is weak: the median pairwise correlation coefficient is 0.09 and the 90th percentile 0.26, even for stations 50–100 km apart. The largest daily totals are evidently produced by individual convective cells and clusters, which is the main reason why the extremes at different stations behave almost as independent samples. This property is favourable both for field-significance testing and for regional pooling.

4.2 Homogeneity

At 24 of the 25 stations none of the three tests, or at most one of them, indicated a change-point at the 5% level. At Belgorod all three tests indicated a shift (most probable year 2003; p = 0.02–0.05); the series was retained, but its trend, which is the most negative in the network, should be read with this in mind. Stary Oskol (Buishand test only, p = 0.02) and Rylsk (standard normal homogeneity test only, p = 0.04) gave isolated indications that we do not regard as decisive. For the 1936–2025 series, Pettitt's test indicated a shift at Kamennaya Step around 1985 (p = 0.04); no step is apparent at any station around 1950–1953, when the Tretyakov gauge replaced the earlier instruments.

4.3 Trends in annual maxima, 1960–2025

Theil–Sen slopes are positive at 14 stations, exactly zero at six and negative at five (Fig. 2a, Table 2). The regional median is + 0.21 mm per decade, or about 0.6% of the long-term mean, with a range from − 1.45 mm per decade at Belgorod to + 1.38 mm per decade at Rylsk. No station is significant at the 5% level after correction for serial correlation, and the two stations closest to significance have opposite signs (Belgorod, –

3.9% per decade, p = 0.05; Yelets, + 3.2% per decade, p = 0.09). Lag-1 autocorrelation is small (median 0.07, maximum 0.35), so that the correction changes the p-values only marginally.

Table 2

Theil–Sen slopes (mm per decade and % of the station mean per decade) and p-values of the Mann–Kendall test corrected for serial correlation for annual, warm-season (April–October) and cold-season (November–March) maximum daily precipitation, 1960–2025. Zero slopes arise from ties in integer-millimetre data

Station	Annual: mm/dec	%/dec	p	Warm: mm/dec	%/dec	p	Cold: mm/dec	%/dec	p
Anna	0.29	0.8	0.79	0.23	0.7	0.81	0.59	3.1	0.15
Belgorod	-1.45	-3.9	0.05	-1.15	-3.2	0.17	0.00	0.0	0.64
Bogoroditskoye	0.74	2.1	0.23	0.74	2.1	0.23	0.68	4.0	0.02
Boguchar	0.00	0.0	0.92	0.27	0.8	0.72	0.00	0.0	0.78
Borisoglebsk	-0.70	-1.9	0.29	-0.24	-0.7	0.79	0.00	0.0	0.99
Valuyki	0.56	1.4	0.55	0.32	0.8	0.67	0.50	2.6	0.24
Voronezh	0.77	2.2	0.18	0.48	1.4	0.42	1.25	6.4	0.02
Gotnya	0.20	0.6	0.67	0.34	1.0	0.64	0.00	0.0	0.91
Yelets	1.19	3.2	0.09	1.25	3.4	0.09	0.42	2.4	0.17
Zherdevka	0.21	0.6	0.73	0.00	0.0	0.79	0.00	0.0	0.91
Kalach	0.61	1.8	0.32	0.48	1.4	0.38	0.26	1.4	0.36
Kamennaya Step	0.75	2.3	0.34	0.67	2.0	0.39	0.50	3.1	0.11
Kirsanov	0.00	0.0	0.98	0.00	0.0	0.86	0.53	3.0	0.11
Kon-Kolodez	0.53	1.5	0.35	0.37	1.1	0.50	1.20	7.0	< 0.01
Kursk	1.02	2.7	0.26	0.78	2.1	0.37	-0.18	-0.9	0.50
Lipetsk	0.77	2.3	0.20	0.88	2.6	0.18	0.00	0.0	1.00
Liski	0.00	0.0	0.81	0.00	0.0	0.87	1.11	6.6	0.02
Michurinsk	0.00	0.0	0.84	0.00	0.0	0.98	0.00	0.0	0.57
Morshansk	0.00	0.0	0.79	0.22	0.7	0.75	0.25	1.5	0.41
Novy Oskol	0.00	0.0	1.00	0.00	0.0	0.92	0.52	3.0	0.15
Oboyan	0.36	1.0	0.74	0.42	1.1	0.64	0.56	2.9	0.19
Ponyri	-0.26	-0.6	0.66	-0.35	-0.8	0.57	0.69	3.9	0.06
Rylsk	1.38	3.4	0.19	1.05	2.6	0.20	0.51	2.4	0.21
Stary Oskol	-1.28	-3.2	0.17	-1.04	-2.7	0.20	0.00	0.0	0.78
Tambov	-0.71	-2.1	0.22	-0.71	-2.1	0.22	-0.22	-1.4	0.47
Median	0.21	0.6		0.27	0.8		0.42	2.4	

The permutation test shows that this pattern is well within the range expected in the absence of any trend: 14 or more positive slopes occurred in 16% of the permutations, a surplus of nine or more positive over negative slopes in 13%, and three or more locally significant stations in 46% (Table 3). The regional series (Fig. 3a) has a Theil–Sen slope of + 1.1% per decade (p = 0.22; permutation p = 0.22). Decadal means describe its course better than a straight line: 34.1 mm in the 1960s, 36.1 mm in the 1970s, 37.9 mm in the 1980s and 38.4 mm in the 1990s, followed by a fall to 35.4 mm in the 2000s and 36.4 and 35.9 mm in the 2010s and in 2020–2025. In relative terms the 1980s–1990s were about 5% above and the 1960s about 6% below the long-term mean.

Table 3
Field significance of station trends, 1960–2025. n+, n0, n− – numbers of positive, zero and negative Theil–Sen slopes; nsig – number of stations significant at the 10% level; p-values from 1000 permutations of calendar years preserving the spatial dependence of the data; the last three columns refer to the regional series (mean of station Rx1day normalised by the station mean)

Series	n+	n0	n−	nsig	p(n+)	p(n+ − n−)	p(nsig)	Regional slope, %/dec	p (MK)	p (perm.)
Annual	14	6	5	3	0.16	0.13	0.46	1.1	0.22	0.22
Warm season (Apr–Oct)	15	5	5	1	0.11	0.11	0.91	1.1	0.16	0.22
Cold season (Nov–Mar)	15	8	2	5	0.10	0.10	0.14	2.0	0.12	0.11

An instructive by-product concerns station selection. The 12 stations with complete or nearly complete records – the kind of subset that would commonly be chosen for a trend study – give 11 positive slopes, one zero and no negative slope for 1960–2022, with a median of + 0.97 mm per decade. The remaining 13 stations, which have gaps in the same years, give six positive, two zero and five negative slopes with a median of zero. The two subsets do not differ systematically in location or elevation; the contrast appears to be a sampling accident, but one that would have produced an apparently coherent regional increase had the analysis been confined to the complete records.

4.4 Seasonal maxima

Warm-season maxima, which coincide with the annual maxima in 93% of station-years, give almost the same picture as the annual series: 15 positive, five zero and five negative slopes, one station significant at the 10% level (Yelets), a regional slope of + 1.1% per decade (p = 0.16) and field p-values of 0.11–0.91 (Table 3).

Cold-season maxima behave differently (Fig. 2b). Slopes are positive at 15 stations, zero at eight and negative at only two; four stations are significant at the 5% level (Voronezh, + 6.4% per decade; Kon-Kolodez, + 7.0%; Liski, + 6.6%; Bogoroditskoye, + 4.0%) and a fifth (Ponyri) at the 10% level. The regional series rises by about 2.0% per decade (Fig. 3b; p = 0.12); the field p-values are 0.10 for the number of positive slopes and 0.14 for the number of locally significant stations. The cold-season signal is thus more coherent than the annual one, although it does not reach conventional significance at the regional scale either, and it concerns events that are on average half as large as the summer maxima and rarely determine the annual value.

4.5 The longer perspective, 1936–2025

At the 12 stations with records from 1936, slopes over 90 years are positive at eight, zero at two and negative at two (Table 4). Two stations are significant at the 5% level – Kamennaya Step (+ 0.91 mm per decade, p = 0.04) and Voronezh (+ 0.76 mm per decade, p = 0.05) – and Michurinsk at the 10% level. At Kamennaya Step the increase takes the form of a step around 1985 rather than a gradual change, and the first thirty years of its record (mean 27.5 mm) are low relative to all other stations. Decadal means of the normalised regional series for the 12 stations are 1.01 in the 1940s and 1950s, 0.94 in the 1960s, 0.98 in the 1970s, 1.06 in the 1980s and 1990s, 1.00 in the 2000s, 1.03 in the 2010s and 0.95 in 2020–2025 (Fig. 3c). The long series therefore place the 1960–2025 period in a context of decadal fluctuations of about ± 6% around a nearly constant level, with the 1960s as a low decade; a linear trend fitted from 1960 onwards partly reflects this starting point.

Table 4
Trends in annual maximum daily precipitation at the 12 long-record stations, 1936–2025: Theil–Sen slope, p-value of the corrected Mann–Kendall test, most probable change-point year and p-value of the Pettitt test, and mean Rx1day for three 30-year sub-periods

Station	n	Slope, mm/dec	%/dec	p	Change-point year	p (Pettitt)	1936–1965	1966–1995	1996–2025
Anna	83	0.00	0.0	0.86	1971	1.00	37.6	36.0	36.1
Belgorod	77	-0.50	-1.4	0.36	2003	0.20	37.3	38.7	35.2
Bogoroditskoye	85	0.00	0.0	0.73	1988	0.96	38.0	33.7	36.9
Boguchar	86	0.48	1.4	0.15	1996	0.71	30.3	35.2	34.7
Valuyki	87	0.41	1.1	0.49	1972	0.28	36.0	37.7	40.4
Voronezh	87	0.75	2.2	0.05	1986	0.07	34.9	34.7	35.5
Gotnya	86	0.19	0.5	0.67	1972	0.26	34.5	35.9	36.6
Kamennaya Step	88	0.91	2.9	0.04	1985	0.04	27.5	32.2	33.7
Kon-Kolodez	86	0.77	2.3	0.12	1978	0.10	30.9	35.1	34.1
Kursk	88	0.40	1.0	0.57	1975	0.62	42.6	36.0	40.5
Michurinsk	82	0.87	2.5	0.10	1974	0.08	30.5	39.2	34.9
Tambov	90	-0.26	-0.8	0.49	2004	0.36	32.8	35.1	32.5

4.6 At-site frequency analysis

The GEV shape parameter (in the sign convention of Hosking 1990) is negative at 21 of the 25 stations (median − 0.09, range − 0.29 to + 0.16), i.e. the upper tail is somewhat heavier than that of the Gumbel distribution at most sites. Neither GEV nor PE3 is rejected by the Kolmogorov–Smirnov test at any station (smallest p = 0.44), and the regional average L-moment ratios (L-skewness 0.22, L-kurtosis 0.16) fall close to the GEV curve on the L-moment ratio diagram (Fig. 4a).

The estimated design values span a wide range across the region (Table 5, Fig. 5). For T = 10 years the GEV estimates lie between 46 and 66 mm (median 53 mm); for T = 50 years between 57 and 101 mm (median 75 mm); and for T = 100 years between 60 and 123 mm (median 86 mm). The PE3 estimates by L-moments are within 1 mm of the GEV at T = 10 years and lower by a median of 3 mm at T = 100 years (range − 0.5 to + 11 mm); PE3 by conventional moments gives values lower again by a few millimetres at the most skewed sites. Bootstrap 90% intervals of the 100-year GEV quantile have a median half-width of 15 mm, or 19% of the point estimate (range 11–33%). The spread of the 100-year values across the region – a factor of two between the lowest and the highest station – is far larger than the spread of the means (a factor of 1.3) and is dominated by differences in sample skewness, which in turn are driven by one or two large events per station; the widest intervals belong to Kalach and Stary Oskol, where the two largest regional values were recorded.

Table 5

Design daily precipitation (mm) for return periods of 10, 50 and 100 years: at-site GEV estimates (L-moments) with 90% bootstrap intervals for T = 100 years, at-site Pearson type III estimates by L-moments (PE3-LM) and by conventional moments (PE3-MM), and regional (index) estimates with 90% intervals. The last column is the ratio of the at-site to the regional 100-year value

Station	GEV T = 10	GEV T = 50	GEV T = 100 (90% CI)	PE3-LM T = 100	PE3-MM T = 100	Reg. T = 10	Reg. T = 50	Reg. T = 100 (90% CI)	Ratio
Anna	53	73	82 (64–101)	79	80	53	73	83 (74–89)	1.01
Belgorod	51	62	65 (56–74)	66	65	55	76	86 (79–90)	1.31
Bogoroditskoye	48	57	60 (53–68)	61	61	52	72	82 (75–85)	1.35
Boguchar	53	78	90 (76–103)	85	79	52	71	80 (72–86)	0.90
Borisoglebsk	54	72	80 (65–94)	77	75	55	76	86 (77–91)	1.08
Valuyki	57	80	91 (72–106)	87	85	58	80	90 (81–96)	0.99
Voronezh	51	68	76 (58–99)	73	80	52	72	82 (73–86)	1.07
Gotnya	54	78	89 (69–105)	84	82	54	74	84 (76–88)	0.94
Yelets	57	81	93 (74–109)	89	85	55	76	86 (76–92)	0.92
Zherdevka	51	73	83 (63–100)	79	79	51	70	80 (72–85)	0.95
Kalach	53	88	108 (72–144)	98	103	50	70	79 (69–86)	0.72
Kamennaya Step	46	58	63 (54–70)	62	60	49	67	76 (69–80)	1.20
Kirsanov	53	75	86 (71–96)	82	77	52	72	81 (73–87)	0.94
Kon-Kolodez	49	65	72 (57–86)	70	71	51	70	79 (72–84)	1.10
Kursk	57	81	92 (77–106)	88	83	57	78	88 (79–94)	0.96
Lipetsk	49	66	74 (57–90)	71	72	50	69	78 (70–82)	1.05

Station	GEV T = 10	GEV T = 50	GEV T = 100 (90% CI)	PE3-LM T = 100	PE3-MM T = 100	Reg. T = 10	Reg. T = 50	Reg. T = 100 (90% CI)	Ratio
Liski	48	65	72 (58–87)	70	69	48	66	75 (67–81)	1.04
Michurinsk	58	81	91 (75–105)	88	84	55	75	85 (74–91)	0.93
Morshansk	50	65	72 (59–83)	70	69	49	68	77 (68–82)	1.07
Novy Oskol	56	78	88 (70–103)	84	82	56	77	87 (78–93)	0.98
Oboyan	56	79	90 (76–98)	85	79	55	76	86 (77–91)	0.96
Ponyri	66	96	110 (95–119)	105	96	63	88	99 (88–106)	0.90
Rylsk	59	80	90 (73–105)	87	86	60	83	94 (85–99)	1.04
Stary Oskol	62	101	123 (93–146)	112	105	58	81	91 (79–99)	0.74
Tambov	48	65	73 (58–87)	70	69	50	69	78 (70–83)	1.06

4.7 Regional frequency analysis

Only Michurinsk exceeds the critical discordancy value (D = 3.3), with Kalach close to it (D = 2.97). The heterogeneity measure H1 = 2.5 classifies the 25-station set as heterogeneous by the criteria of Hosking and Wallis (1997), whereas H2 = − 0.8 and H3 = − 1.0 lie within the range expected for a homogeneous region. Because H2 and H3 are known to have little power to detect heterogeneity (Hosking and Wallis 1997), the three values are best read together as indicating that the dispersion of L-CV among sites is larger than sampling alone would produce, while the shape of the distribution, described by L-skewness and L-kurtosis, varies no more than expected. The heterogeneity therefore arises from the dispersion of L-CV (0.15–0.25 across sites), which in a region without an apparent climatic gradient in the mean is most plausibly a mixture of sampling variability – the L-CV of a 60-year sample of a skewed variable is itself uncertain by roughly ± 0.03 – and genuine differences in gauge exposure and microrelief that the available metadata cannot resolve. Among the candidate distributions, the generalised normal (Z = 0.31), the GEV (Z = 1.40) and the PE3 (Z = − 1.75, marginally outside the acceptance interval) are compatible with the regional L-moments, while the generalised logistic is not (Z = 4.65). We adopt the GEV growth curve for comparability with the at-site analysis; its parameters are ξ = 0.823, α = 0.265 and k = − 0.083, giving growth factors of 1.48, 1.72, 2.04 and 2.31 for T = 10, 20, 50 and 100 years (Fig. 4b, Table 6). Removing Michurinsk alone lowers H1 to 2.1, and removing the three most discordant sites (Michurinsk, Kalach and Bogoroditskoye) to 1.0, i.e. to the boundary between ‘acceptably homogeneous’ and ‘possibly heterogeneous’. The 22-site subset reduces the 100-year

growth factor to 2.24 (− 3%) and changes the site quantiles by a median of 7%, so the conclusions do not hinge on these stations; at the same time, a substantial part of the apparent heterogeneity appears to be contributed by two or three sites with unusually heavy or light upper tails.

Table 6
Regional growth factors (quantile divided by the station mean) of the regional GEV distribution for the 25-station region, with 90% bootstrap intervals, and for the 22-station subset without the three most discordant sites. Heterogeneity measures for the 25 sites: H1 = 2.5, H2 = − 0.8, H3 = − 1.0 (H1 = 2.1 without Michurinsk, 1.0 for the 22-site subset). Goodness-of-fit measures Z: generalised logistic 4.65, GEV 1.40, generalised normal 0.31, PE3 − 1.75

Return period T, years	Growth factor (25 sites)	90% interval	Growth factor (22 sites)
2	0.922	–	0.928
5	1.247	–	1.243
10	1.479	1.456–1.488	1.466
20	1.716	–	1.689
50	2.045	1.953–2.068	1.995
100	2.308	2.175–2.343	2.237
200	2.585	–	2.489

Regional 100-year estimates range from 75 mm (Liski) to 99 mm (Ponyri) with a median of 83 mm, i.e. the range is halved relative to the at-site estimates (Table 5, Fig. 5). Their 90% intervals have a median half-width of 7 mm (about 8%), compared with 15 mm (19%) for the at-site estimates. At 18 of the 25 stations the at-site and regional 100-year values agree within 10%; the largest departures are at Kalach and Stary Oskol (at-site values 28–30% above the regional ones) and at Belgorod and Bogoroditskoye (at-site values about 25% below). Whether these departures reflect real local differences or sampling effects cannot be decided from 60-year records; the regional estimate is, in our view, the more defensible design value, with the at-site estimate serving as an indication of local uncertainty.

4.8 Trend magnitude compared with estimation uncertainty

The 100-year GEV quantile estimated from the second half of the record exceeds that from the first half at 13 of the 25 stations; the median difference is + 0.6 mm, with individual differences from − 39 to + 30 mm that are dominated by the presence or absence of a single large event in one half. The non-stationary GEV improves on the stationary model at the 5% level at two stations (Belgorod and Rylsk, with slopes of opposite sign), which is about the number expected by chance among 25 tests; the location parameter increases with time at 16 stations, and the implied change of the effective 100-year value between 1960 and 2025 has a median of + 0.7 mm and a range of − 9 to + 9 mm. Both experiments give the same answer: the change in design values that can be attributed to the observed trends is an order of magnitude smaller than the sampling uncertainty of the stationary estimates (about ± 15 mm at-site and ± 7 mm regional).

The power calculation explains why. For series of 64 years with the variability observed in the region, the Mann–Kendall test at the 5% level detects a trend of 0.5 mm per decade with a probability of about 10%, 1

mm per decade with 23%, 2 mm per decade with 71% and 3 mm per decade with 95%. A change of 1–1.5% of the mean per decade – the order of magnitude suggested by the regional series – is therefore below the detection threshold of individual stations and close to it for the network as a whole.

5 Discussion

5.1 No detectable regional intensification – and what this does and does not mean

The main result of the trend analysis is negative: annual maximum daily precipitation in the CCR shows no change over 1960–2025 that can be distinguished from chance, neither at individual stations nor as a field, and the nine-decade records point to decadal fluctuations around a nearly constant level rather than to a sustained trend. The sign of the regional slope is positive and its magnitude (about 1% per decade) is not inconsistent with the hemispheric tendency (Westra et al. 2013; Sun et al. 2021), but the same data are equally consistent with no change at all. We would therefore hesitate to describe the region as one of emerging intensification: the more appropriate statement is that an increase of up to about 2% per decade cannot be excluded, while a larger one appears unlikely.

Two features of the analysis deserve emphasis because they bear on how similar regional studies should be read. First, the apparent coherence of trends depends strongly on which stations are included: the complete records alone would have suggested a uniform increase that the full network does not support. Selection by record completeness is common practice and is not wrong in itself, but with a dozen stations the risk of such a sampling accident is real, and the full network combined with a field-significance test provides a safeguard. Second, the absence of significance should not be mistaken for evidence of stability. The power calculation shows that trends of the magnitude plausibly expected from thermodynamic scaling – about 7% per kelvin, i.e. 2–3% per decade for a regional warming of 0.3–0.4 K per decade (Trenberth et al. 2003) – would be detected at individual stations in only a minority of cases. Longer records, denser networks and sub-daily data will be needed before the question can be settled; in the meantime, the field-level result is the more informative one.

5.2 Physical context

Several factors may explain why the CCR does not show the increase documented for Russia as a whole. The national signal is strongest for the share of convective precipitation in seasonal totals and for extremes in the northern and central parts of European Russia (Chernokulsky et al. 2019; Aleshina et al. 2021). In the forest-steppe, summer precipitation has not increased; warm, dry summers have become more frequent, and the 2000s – the decade with the lowest regional Rx1day since the 1960s – include the exceptional heat and drought of 2010 (Barriopedro et al. 2011). Convective intensity depends not only on temperature but on available moisture and on soil-moisture feedbacks (Berg et al. 2013), and in a region on the edge of the semi-arid zone the thermodynamic increase in potential rainfall intensity may be partly offset by less frequent triggering of deep convection in dry summers. The sequence of a wet 1980s–1990s and a dry 2000s is also consistent with low-frequency variability of the large-scale circulation rather than with a monotonic forced

response. We offer these as plausible explanations rather than as demonstrated causes; the data analysed here cannot separate them.

5.3 The cold-season signal

The more coherent increase of cold-season maxima is in line with the strong winter warming of European Russia, which has increased the frequency of liquid and mixed precipitation and of thaw events in November–March (Roshydromet 2022). From the point of view of hazards the change is secondary – cold-season maxima are small and rarely set the annual value – but it is not negligible for erosion, because rainfall on frozen or saturated soil generates efficient runoff, and because rain-on-snow events can produce the largest spring discharges from small catchments. A dedicated analysis of cold-season liquid precipitation, which requires daily temperature and precipitation-type information, would be a logical continuation.

5.4 Implications for design values

For design purposes, three practical conclusions follow. (1) The uncertainty of at-site 100-year daily precipitation in the region, about ± 19% for 60-year records, is large enough to matter and should be reported alongside the point estimate. (2) Regional estimation reduces this uncertainty by more than half and removes much of the implausible station-to-station variability; a single regional growth curve with the station mean as index appears to be a defensible basis for design in the CCR, and the heterogeneity statistics suggest that any further subdivision should be guided by L-CV rather than by the shape of the distribution. (3) Non-stationarity is not, at present, a measurable component of design uncertainty for daily maxima in this region: the trend-related changes are an order of magnitude smaller than the sampling uncertainty, so that a stationary estimate with explicit uncertainty bounds appears adequate, provided it is periodically updated (Serinaldi and Kilsby 2015; cf. Milly et al. 2008). This does not contradict the general expectation of intensification under continued warming; it reflects the detection limits of the available records and the modest size of any change relative to natural variability. For the small catchments of the region, moreover, design rainfall is only one of several inputs: changes in land use and in the condition of the landscape influence the maximum discharge alongside changes in storm rainfall (Ilinich et al. 2020, 2023), and the two need to be assessed together.

The choice of distribution is of secondary importance at return periods up to 50 years, but at 100 years the PE3 fitted by conventional moments gives lower values than the GEV at the most skewed sites, by up to 10–15%. Given that the regional L-moments favour distributions with a heavier-than-Gumbel tail, the conventional PE3 estimates may be slightly on the low side for the longest return periods.

5.5 Limitations

Station density remains the principal limitation: 25 stations over 168 000 km² cannot resolve the spatial structure of convective extremes, and the field-significance test is conditioned on the available network. Daily totals from fixed observation windows underestimate true 24-hour maxima by a factor of about 1.1 (Papalexiou et al. 2016); this affects absolute design values but not trends. Integer-millimetre reporting produces ties and zero slopes but does not bias the sign of trends. Gauge exposure and wetting corrections may have changed at individual stations, and the Belgorod series in particular shows signs of inhomogeneity that we could not attribute. Finally, the regional procedure assumes that the stations share a common growth

curve; the H1 statistic indicates that this holds only approximately, and the regional estimates should be read as a reasonable compromise rather than as the final word.

6 Conclusions

1. Over 1960–2025, annual maximum daily precipitation at 25 stations of the Central Chernozem Region shows Theil–Sen slopes with a regional median of +0.2 mm per decade (0.6 % of the mean); no station is significant at the 5 % level, the ensemble of station trends is not field-significant, and the 1936–2025 records show decadal fluctuations of about ±6 % around a nearly constant level.

2. A more coherent increase, of about 2 % per decade, is found for cold-season maxima, which are about half as large as the summer maxima and rarely determine the annual value.

3. At-site 100-year daily precipitation ranges from 60 to 123 mm with 90 % bootstrap intervals of about ±19 %; regional frequency analysis based on L-moments narrows the range to 75–99 mm and the intervals to about ±8 %. The region is moderately heterogeneous in L-CV but homogeneous in the shape of the distribution; the GEV and generalised normal distributions fit the regional L-moments best.

4. Changes in the 100-year quantile implied by the observed trends (median below 1 mm) are an order of magnitude smaller than the estimation uncertainty. For current design practice in the region, stationary regional estimates with explicit uncertainty bounds appear adequate; the lack of a detectable trend reflects the limited statistical power of 60-year station records rather than evidence that extremes are not changing.

5. The quality-controlled station dataset of annual and seasonal maxima, provided as supplementary material, can serve as a benchmark for evaluating gridded and reanalysis precipitation extremes over this part of European Russia.

Declarations

Acknowledgements The author thanks the All-Russian Research Institute of Hydrometeorological Information – World Data Centre for open access to station data.

Funding The author received no specific funding for this work.

Competing interests The author declares no competing interests.

Data availability Daily precipitation data of Roshydromet stations are available from RIHMI-WDC (http://meteo.ru). The annual and seasonal maximum series used in this study and the results of all tests are provided as Electronic Supplementary Material (ESM 1, spreadsheet).

Author contributions Single-author study: conceptualisation, data compilation, analysis, writing and revision were carried out by the author.

Ethics approval Not applicable.

References

1. Aleshina MA, Semenov VA, Chernokulsky AV (2021) A link between surface air temperature and extreme precipitation over Russia from station and reanalysis data. Environ Res Lett 16:105004
2. Alexandersson H (1986) A homogeneity test applied to precipitation data. J Climatol 6:661–675
3. Barriopedro D, Fischer EM, Luterbacher J, Trigo RM, García-Herrera R (2011) The hot summer of 2010: redrawing the temperature record map of Europe. Science 332:220–224
4. Berg P, Moseley C, Haerter JO (2013) Strong increase in convective precipitation in response to higher temperatures. Nat Geosci 6:181–185
5. Buishand TA (1982) Some methods for testing the homogeneity of rainfall records. J Hydrol 58:11–27
6. Bulygina ON, Razuvaev VN, Korshunova NN, Shvets NV (2014) Description of the data set of daily precipitation at Russian stations. RIHMI-WDC, Obninsk. http://meteo.ru/data. Accessed [date]
7. Castellarin A, Burn DH, Brath A (2008) Homogeneity testing: how homogeneous do heterogeneous cross-correlated regions seem? J Hydrol 360:67–76
8. Chernokulsky A, Kozlov F, Zolina O, Bulygina O, Mokhov II, Semenov VA (2019) Observed changes in convective and stratiform precipitation in Northern Eurasia over the last five decades. Environ Res Lett 14:045001
9. Coles S (2001) An introduction to statistical modeling of extreme values. Springer, London
10. Donat MG, Lowry AL, Alexander LV, O'Gorman PA, Maher N (2016) More extreme precipitation in the world's dry and wet regions. Nat Clim Change 6:508–513
11. Fowler HJ, Lenderink G, Prein AF, Westra S, Allan RP, Ban N, Barbero R, Berg P, Blenkinsop S, Do HX, Guerreiro S, Haerter JO, Kendon EJ, Lewis E, Schaer C, Sharma A, Villarini G, Wasko C, Zhang X (2021) Anthropogenic intensification of short-duration rainfall extremes. Nat Rev Earth Environ 2:107–122
12. Groisman PY, Koknaeva VV, Belokrylova TA, Karl TR (1991) Overcoming biases of precipitation measurement: a history of the USSR experience. Bull Am Meteorol Soc 72:1725–1733
13. Groisman PY, Knight RW, Easterling DR, Karl TR, Hegerl GC, Razuvaev VN (2005) Trends in intense precipitation in the climate record. J Clim 18:1326–1350
14. Hamed KH, Rao AR (1998) A modified Mann–Kendall trend test for autocorrelated data. J Hydrol 204:182–196
15. Hosking JRM (1990) L-moments: analysis and estimation of distributions using linear combinations of order statistics. J R Stat Soc Ser B 52:105–124
16. Hosking JRM, Wallis JR (1997) Regional frequency analysis: an approach based on L-moments. Cambridge University Press, Cambridge
17. Ilinich V, Perminov A, Belolybcev A, Naumova A (2020) Assessment of the impact of changes in storm rainfall and landscape characteristics on the maximum flow of small rivers. In: Gourbesville P, Caignaert G (eds) Advances in hydroinformatics: SimHydro 2019 – models for extreme situations and crisis management. Springer Water. Springer, Singapore, pp 717–725. https://doi.org/10.1007/978-981-15-5436-0_55

18. Ilinich VV, Perminov AV, Naumova AA (2023) Influence of landscape and climate changes on the maximum discharge of small catchment areas. Power Technol Eng 56:635–638. https://doi.org/10.1007/s10749-023-01565-1
19. Katz RW, Parlange MB, Naveau P (2002) Statistics of extremes in hydrology. Adv Water Resour 25:1287–1304
20. Kendall MG (1975) Rank correlation methods, 4th edn. Griffin, London
21. Litvin LF, Kiryukhina ZP, Krasnov SF, Dobrovol'skaya NG (2017) Dynamics of agricultural soil erosion in European Russia. Eurasian Soil Sci 50:1344–1353
22. Livezey RE, Chen WY (1983) Statistical field significance and its determination by Monte Carlo techniques. Mon Weather Rev 111:46–59
23. Mal'tsev KA, Yermolaev OP (2020) Assessment of soil loss by water erosion in small river basins in Russia. Catena 195:104726
24. Mann HB (1945) Nonparametric tests against trend. Econometrica 13:245–259
25. Milly PCD, Betancourt J, Falkenmark M, Hirsch RM, Kundzewicz ZW, Lettenmaier DP, Stouffer RJ (2008) Stationarity is dead: whither water management? Science 319:573–574
26. Nearing MA, Pruski FF, O'Neal MR (2004) Expected climate change impacts on soil erosion rates: a review. J Soil Water Conserv 59:43–50
27. Papalexiou SM, Montanari A (2019) Global and regional increase of precipitation extremes under global warming. Water Resour Res 55:4901–4914
28. Papalexiou SM, Dialynas YG, Grimaldi S (2016) Hershfield factor revisited: correcting annual maximum precipitation. J Hydrol 542:884–895
29. Pettitt AN (1979) A non-parametric approach to the change-point problem. J R Stat Soc Ser C 28:126–135
30. Roshydromet (2022) Third assessment report on climate change and its consequences in the Russian Federation. Naukoemkie Tekhnologii, St Petersburg (in Russian)
31. Sen PK (1968) Estimates of the regression coefficient based on Kendall's tau. J Am Stat Assoc 63:1379–1389
32. Serinaldi F, Kilsby CG (2015) Stationarity is undead: uncertainty dominates the distribution of extremes. Adv Water Resour 77:17–36
33. SP 33-101-2003 (2004) Determination of design hydrological characteristics. Gosstroy of Russia, Moscow (in Russian)
34. Sun Q, Zhang X, Zwiers F, Westra S, Alexander LV (2021) A global, continental, and regional analysis of changes in extreme precipitation. J Clim 34:243–258
35. Theil H (1950) A rank-invariant method of linear and polynomial regression analysis. Proc K Ned Akad Wet 53:386–392, 521–525, 1397–1412
36. Trenberth KE, Dai A, Rasmussen RM, Parsons DB (2003) The changing character of precipitation. Bull Am Meteorol Soc 84:1205–1217
37. Westra S, Alexander LV, Zwiers FW (2013) Global increasing trends in annual maximum daily precipitation. J Clim 26:3904–3918

38. Wilks DS (2006) On "field significance" and the false discovery rate. J Appl Meteorol Climatol 45:1181–1189
39. Wilks DS (2016) "The stippling shows statistically significant grid points": how research results are routinely overstated and overinterpreted, and what to do about it. Bull Am Meteorol Soc 97:2263–2273
40. Yue S, Pilon P, Cavadias G (2002a) Power of the Mann–Kendall and Spearman's rho tests for detecting monotonic trends in hydrological series. J Hydrol 259:254–271
41. Yue S, Pilon P, Phinney B, Cavadias G (2002b) The influence of autocorrelation on the ability to detect trend in hydrological series. Hydrol Process 16:1807–1829
42. Zhang X, Alexander L, Hegerl GC, Jones P, Klein Tank A, Peterson TC, Trewin B, Zwiers FW (2011) Indices for monitoring changes in extremes based on daily temperature and precipitation data. WIREs Clim Change 2:851–870
43. Zolina O, Simmer C, Gulev SK, Kollet S (2010) Changing structure of European precipitation: longer wet periods leading to more abundant rainfalls. Geophys Res Lett 37:L06704

Figures

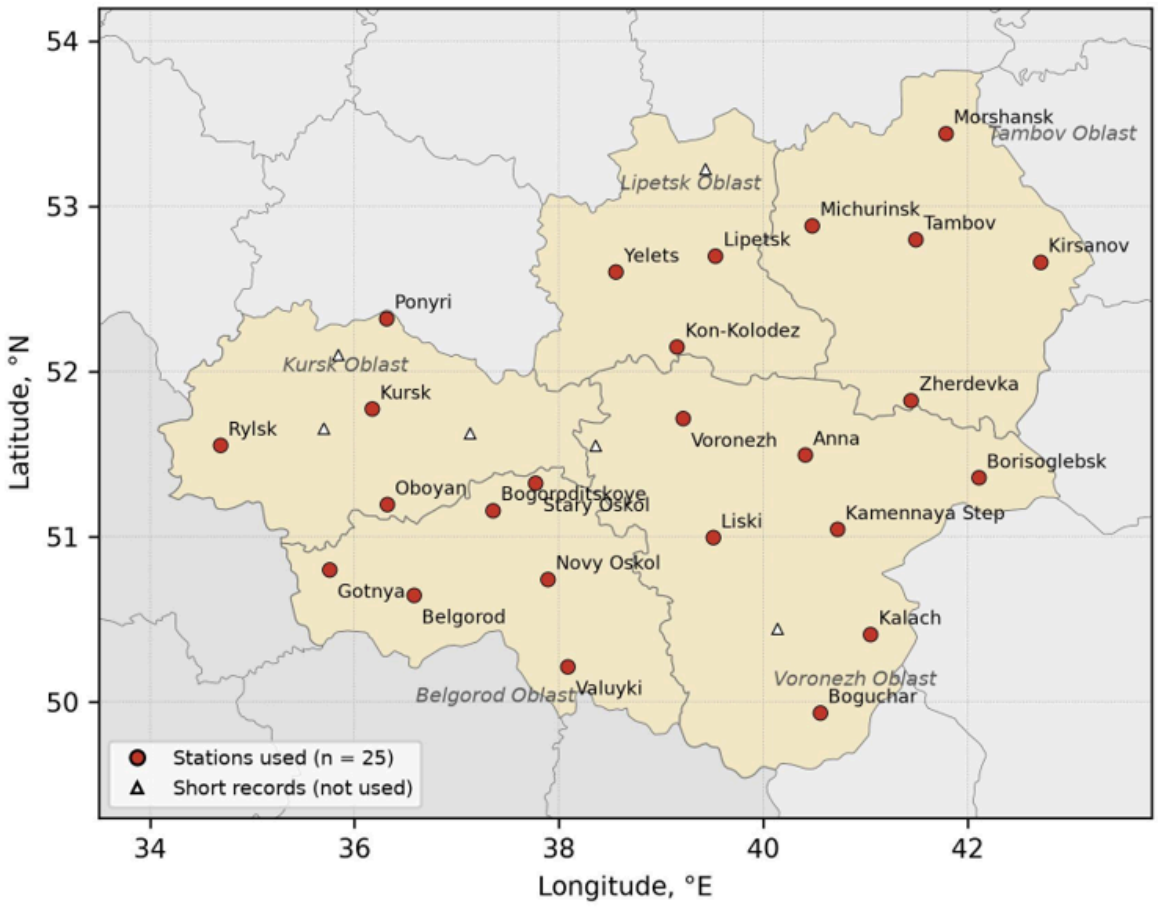


Figure 1

Location of the 25 meteorological stations of the Central Chernozem Region used in the study (filled circles). Open triangles mark stations with short records (from 2000–2011) that were not used. The shaded area shows the Belgorod, Kursk, Lipetsk, Voronezh and Tambov administrative regions; thin grey lines are the boundaries of neighbouring regions

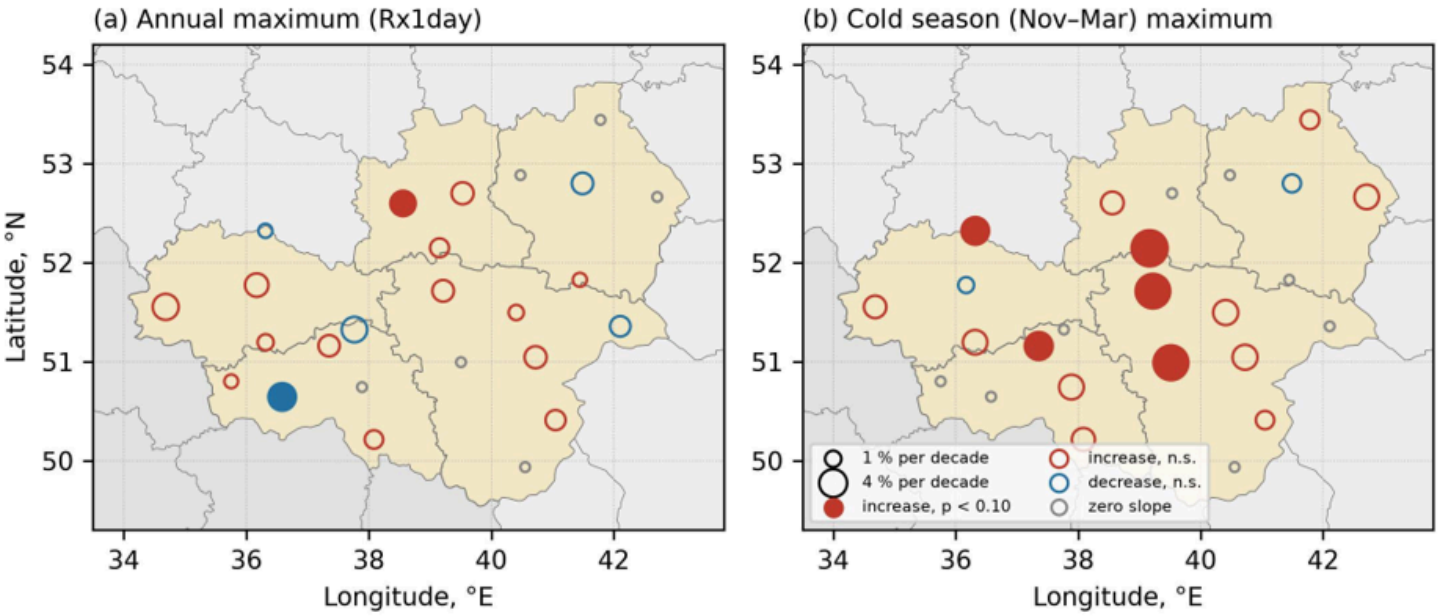


Figure 2

Theil–Sen slopes of maximum daily precipitation at the 25 stations, 1960–2025: (a) annual maximum (Rx1day), (b) cold-season (November–March) maximum. Symbol area is proportional to the slope expressed in per cent of the station mean per decade (reference symbols: 1 % and 4 % per decade); red denotes positive and blue negative slopes, grey symbols mark stations with a zero median slope. Filled symbols indicate slopes significant at the 10 % level of the Mann–Kendall test corrected for serial correlation; open symbols are not significant (n.s.)

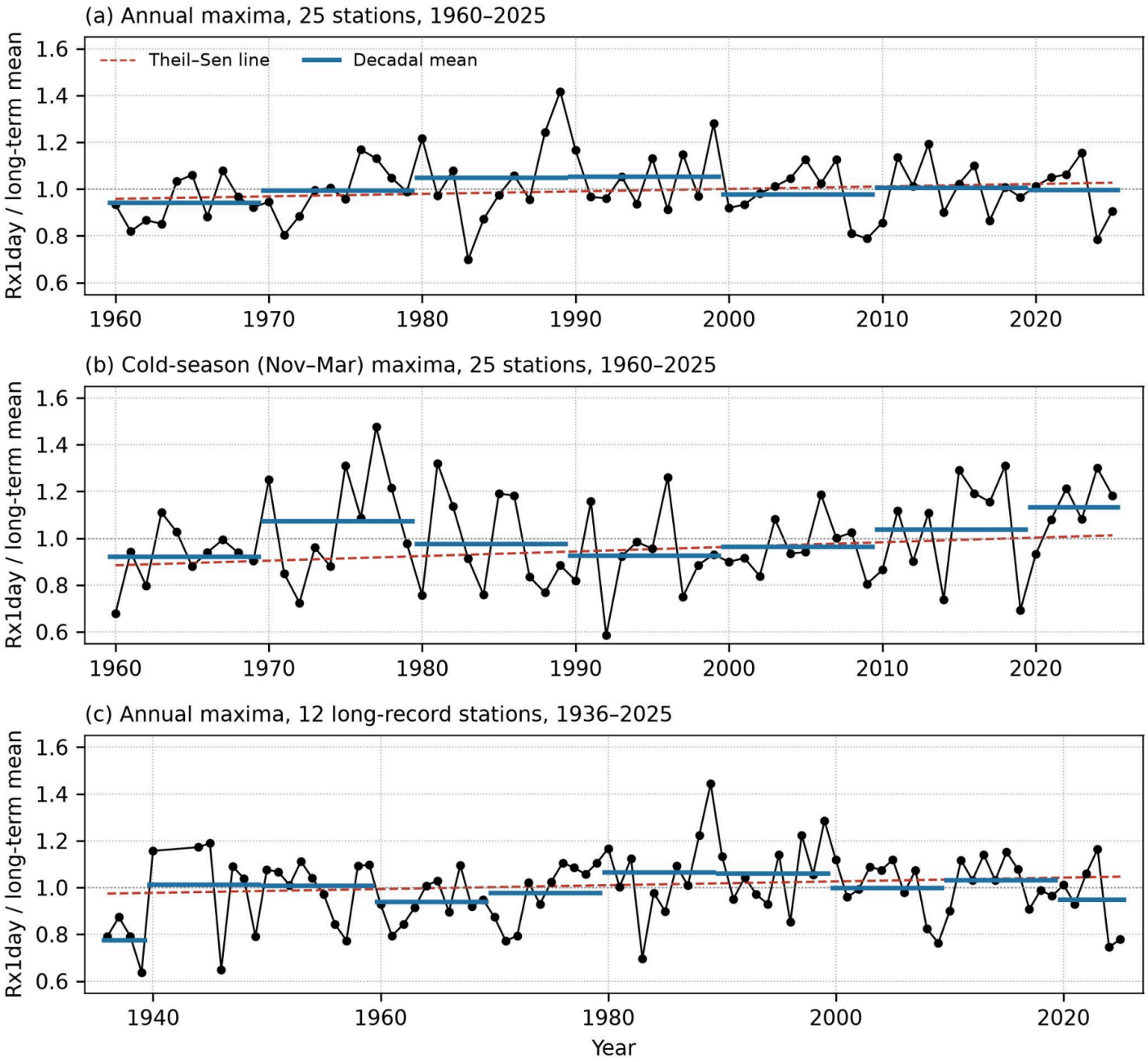


Figure 3

Regional series of maximum daily precipitation (mean over stations of the station value divided by its long-term mean) with Theil–Sen trend lines and decadal means: (a) annual maxima (Rx1day), 25 stations, 1960–2025; (b) cold-season (November–March) maxima, 25 stations, 1960–2025; (c) annual maxima, 12 long-record stations, 1936–2025

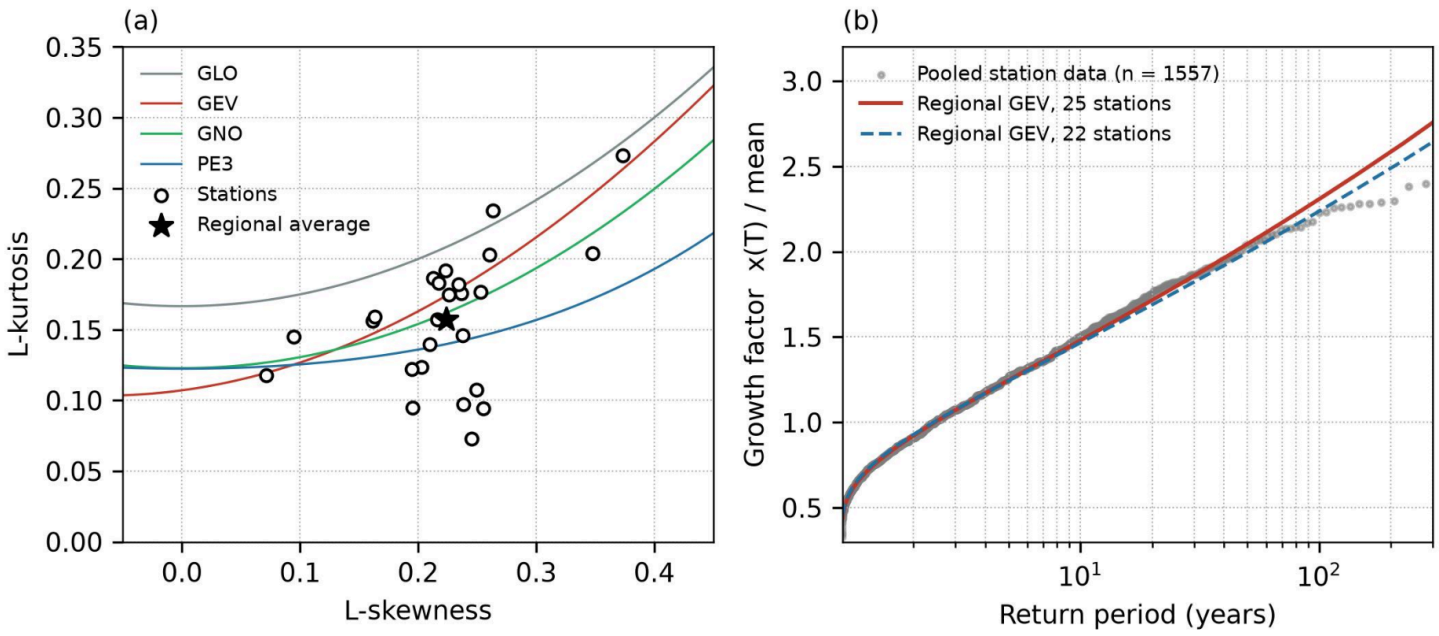


Figure 4

(a) L-moment ratio diagram: sample L-skewness and L-kurtosis of the 25 stations (circles) and their regional average (large symbol) together with the theoretical curves of the generalised logistic (GLO), generalised extreme value (GEV), generalised normal (GNO) and Pearson type III (PE3) distributions; (b) regional GEV growth curves fitted to all 25 stations and to the 22-station subset, compared with the pooled standardised station data (1557 station-years) plotted at their empirical return periods

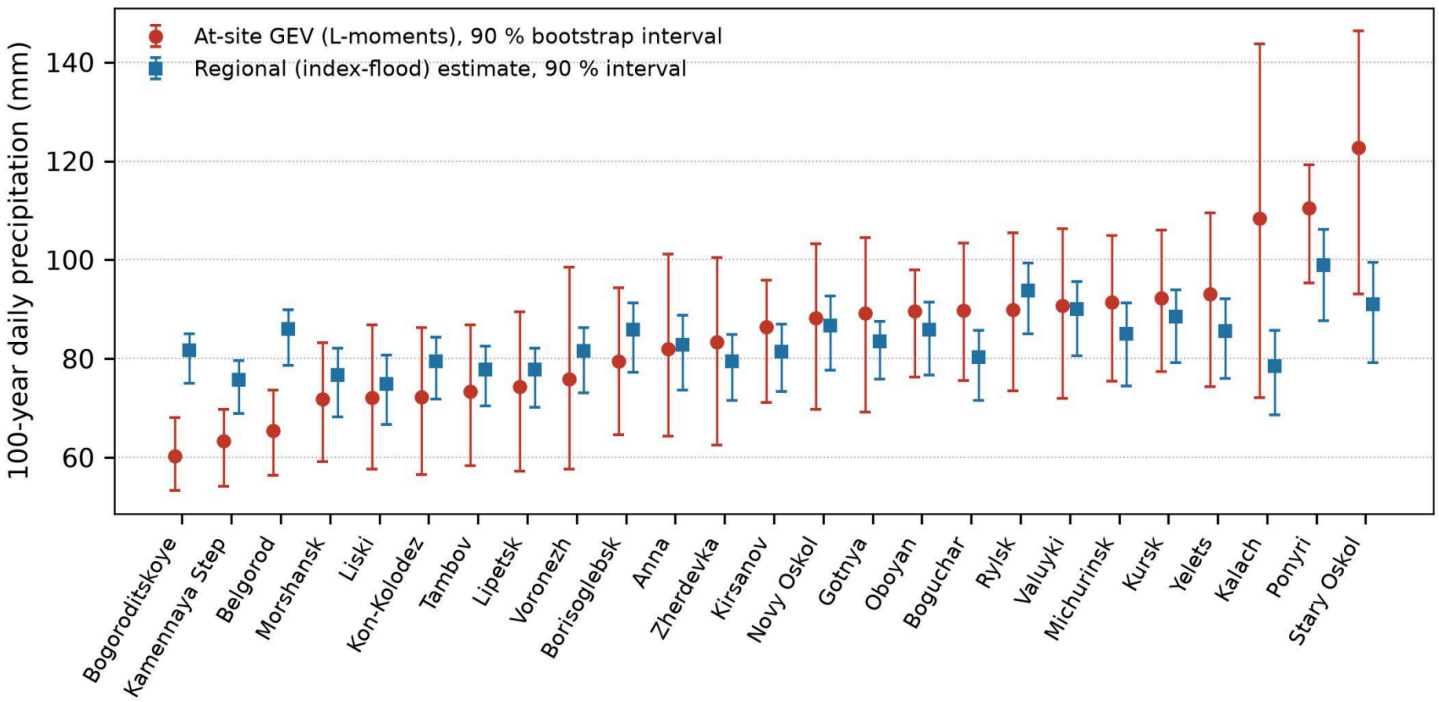


Figure 5

100-year daily precipitation at the 25 stations: at-site GEV (L-moments) estimates with their 90 % bootstrap intervals and regional index-flood estimates with their 90 % intervals

Supplementary Files

This is a list of supplementary files associated with this preprint. Click to download.

- ESM1dataandresults.xlsx